# Theory of epitaxy at finite temperatures: An application to orientational phase transformations on reconstructed Au(001) surfaces

Sun M. Paik
*Department of Physics, Kangwon National University, Chunchon 200-701, Korea*

Jin M. Choi
*Department of Physics, Yonsei University, Seoul 120-650, Korea*

Sung M. Yoo
*Department of Physics, Kangwon National University, Chunchon 200-701, Korea*

Chung N. Whang
*Department of Physics, Yonsei University, Seoul 120-650, Korea*

(Received 31 October 1997)

A new finite temperature epitaxy theory has been introduced which allows us to study epitaxy in systems with nonadditive many-body potentials in finite temperatures. This method is applied to hexagonally reconstructed Au(001) surfaces. We find rotated domains on the surfaces with rotation angles $\theta \approx 0.72°$, 0.86°, and 1.14°, depending on cluster size and shape. These rotated domains undergo orientational phase transformations at temperatures below the melting temperature. We predict that the orientational phase transformations may be accompanied by a reconstruction pattern transformation. [S0163-1829(98)05915-3]

Epitaxial growth has been accomplished experimentally in a large number of systems including lattice-matched and mismatched systems.[1–3] Recent advent of experimental techniques has made it possible to observe the structure of epitaxial systems in microscopic level and various physical phenomena on such systems. A number of theoretical efforts in the literature has been made based on phenomenological models,[4,5] numerical simulations,[6,7] and *ab initio* calculations.[8] However, in many cases, these methods are not able to predict satisfactorily the energetics of epitaxy, especially as a function of system size and temperature. The size of systems and simulation times that can be studied by a numerical simulation or an *ab initio* calculation are much too small to be realistic. On the other hand, phenomenological models can handle much larger systems but have been limited to zero-temperature calculation (rigid model). Moreover, they have employed the two-body additive interaction potentials that cannot predict an accurate surface energy (and epitaxial energy at the same token). Here we present a computational method which allows a systematic calculation of epitaxial energy of large-sized commensurate and incommensurate systems in finite temperatures. This technique is then applied to Au(001) surface reconstruction. We find rotated domains with rotation angles $\theta \approx 0.72°$, 0.86°, and 1.14° due to epitaxial matching effects. The rotated domains undergo phase transformations at temperatures below the bulk melting temperature $T_m$. We predict that these phase transitions may be accompanied by a reconstruction pattern transformation from $(5\times m)$ to $(5\times m')$ where $m$ and $m'$ are integers between 20 and 30. These findings are, to the best of our knowledge, the first comprehensive theoretical predictions of the rotated domains and their phase transformations.

An epitaxial configuration is obtained when free energy of the system is minimum at a coherent lattice-matching situation. Here the coherent lattice-matching situation occurs when lattice constant ratio $\xi_c$ $(=b_a/b_s)$ becomes a rational number in a one-dimensional interface where $b_a$ and $b_s$ are lattice constants of overlayer and substrate lattices, respectively (for two-dimensional interfaces, it also depends on relative orientation $\theta$). At zero temperature with two-body additive potential, obtaining an epitaxial configuration is reduced to finding minimum overlayer-substrate $(a-s)$ interaction[5] which can be written as $V_{a-s} = \Sigma_{\xi_c} \Sigma_{\vec{G}} V_{\vec{G}}(\xi_c)\, \delta_{N_a,\vec{G}}(|\xi - \xi_c|)$, where a set of $\{\vec{G}\}$ are two-dimensional (2D) substrate surface reciprocal lattice vectors, $V_{\vec{G}}$ is the 2D Fourier transform of the interaction potential, $N_a$ is a number of the overlayer atoms, and $\delta_{N_a,\vec{G}}$ is a $\delta$ function in the limit of $N_a \to \infty$. However, in a more realistic model with nonadditive interaction potential, the free energy cannot be written in a simple form as above. Furthermore, in finite temperature calculations, the magnitude of the coherent matching peaks are temperature dependent. Thus epitaxial configurations at finite temperatures may differ significantly from the zero-temperature one. Although a quantitative understanding of thermodynamic behaviors of the epitaxial systems is very important for epitaxial growth, no clear-cut theoretical scheme utilizing more accurate nonadditive many-body potentials at finite temperatures has emerged.

In this paper, we introduce a theoretical method to study epitaxy at finite temperatures that addresses the issues raised above. The assumptions in this method are the following: (1) lattice structure is maintained at all temperatures below the melting temperature although the lattice can be expanded, contracted, and distorted homogeneously; and (2) effects due to local lattice defects such as vacancies, interlayer atomic mixing, and local distortion are negligible (however, global homogeneous lattice distortion, and sinusoidal corrugation

 

and buckling are allowed). Clearly, there are many local lattice defects, intermixing, and surface roughening in a real system. However, effects of these irregularities on average interfacial energy are much smaller than the lattice-matching effects which will be added up coherently at an epitaxial configuration. (Otherwise the system may be too rough to be an epitaxial system.) In actual calculations these irregularity effects are partially included by introducing two adjustable parameters. As an example, we study Au(001) surface reconstruction and orientational phase transformations on the reconstructed surfaces. However, our methodology is quite general and can readily be applied to any epitaxial systems.

The stable equilibrium configuration of a system at a finite temperature can be found by minimizing free energy of the system. The total free energy of an epitaxial system is written as

$$F^{(\mathrm{tot})}=F_s^{(\mathrm{vib})}+\Phi_s+F_a^{(\mathrm{vib})}+\Phi_{\mathrm{int}}, \tag{1}$$

where $F_s^{(\mathrm{vib})}$, $\Phi_s$, $F_a^{(\mathrm{vib})}$, and $\Phi_{\mathrm{int}}$ are vibrational free energy of the substrate, static interaction energy of the substrate, vibrational free energy of the overlayer, and static interfacial energy, respectively. The vibrational free energies $F^{(\mathrm{vib})}(\vec{b})=k_BT\Sigma_{\vec{k},\sigma}\ln\{2\sinh[\hbar\omega_\sigma(\vec{k},\vec{b})/2k_BT]\}$ can easily be calculated as a function of corresponding lattice constants within the quasiharmonic approximation[9] where $k_B$ is Boltzmann constant, $\sigma$ is an index for phonon modes, and $\omega_\sigma(\vec{k},\vec{b})$ is the phonon frequency of the appropriate lattice.

The static energy of the substrate $\Phi_s$ is interaction energy between the substrate atoms when no overlayer is present, and can be calculated using the embedded atomic method (EAM) -type many-body potential,[10,11]

$$U_i=E_i[\rho(\vec{r}_i)]+\frac{1}{2}\sum_{j\neq i}^{N}V_{ij}(r_{ij}), \tag{2}$$

where $N$, $E_i[\rho]$, $\rho(\vec{r}_i)$, and $V_{ij}(r_{ij})$ are the number of atoms, a universal energy functional for the $i$th type of atom, a local electron charge density at the position of the $i$th atom from neighboring atoms, and a two-body repulsive potential, respectively, and $r_{ij}=|\vec{r}_i-\vec{r}_j|$. In a homogeneous substrate lattice all the substrate atoms except the ones in the interface have the same interaction energy and, consequently, the substrate static energy $\Phi_s$ becomes just the number of substrate atoms $N_s$ times the interaction energy of each substrate atom $U_i$.

For the atoms in the interface, the interaction potential cannot be readily summed up to calculate the static interfacial energy $\Phi_{\mathrm{int}}$. To calculate the static interfacial energy we use the same method that has been employed in the zero-temperature calculations with the two-body additive interaction potentials.[5] In this method we utilize the lattice periodicity, and the charge density and the two-body potential are written in terms of Fourier series. Using these Fourier series and the fact that the energy functional $E_i$ is written in a form of a spline fit[10,11] (all we need here is an *expandable function*), the $\Phi_{\mathrm{int}}$ is written as

$$\Phi_{\mathrm{int}}=\Phi_a(\vec{b}_a)+\sum_{\vec{G}}[V_{\vec{G}}(z)+\Gamma_{\vec{G}}(z,\rho_{aa})]\Delta_a(N_a,\vec{b}_a,\vec{G},\theta)+\sum_{\vec{K}}\Gamma_{\vec{K}}(z,\rho_{ss})\Delta_s(N_s,\vec{b}_s,\vec{K},-\theta), \tag{3}$$

where $\vec{K}$, $N_s$, and $z$ are the two-dimensional surface reciprocal lattice vectors of the overlayer lattices, the number of the substrate atoms, and the interface layer distance, respectively. The $\Phi_a(\vec{b}_a)$ is interaction energy between atoms on an isolated overlayer (i.e., without the substrate lattice). The $\rho_{aa}$ ($\rho_{ss}$) is the local electron charge density at an atomic site of the isolated overlayer (substrate) lattice. The functions $\Delta_a$ and $\Delta_s$ are the geometric functions which depend on size and geometry of the overlayer cluster. The geometric functions for various overlayer geometries can be found in Ref. 5. The function $\Gamma_{\vec{G}}(z,\rho_{aa})$ is written as $\Gamma_{\vec{G}}(z,\rho_{aa})=\rho_{\vec{G}}(z)\Sigma_{l=1}^{\infty}(1/l!)E_a^{(l)}[\rho_{aa}][\Sigma_{\vec{G}'}\rho_{\vec{G}'}(z)]^{l-1}$, where the superscript $(l)$ in the functional $E[\rho]$ denotes the $l$th derivative. The $\Gamma_{\vec{K}}(z,\rho_{ss})$ is written in the same manner. These functions are due to the nonadditivity of our interaction potential and, thus, did not appear in the previous additive potential model calculations.[5] Further details of this method will be discussed elsewhere.[12]

As an application of this technique we study thermal behaviors of reconstructed Au(001) surfaces. The EAM type ''glue'' potential[11] is used for the interaction between Au atoms. The hexagonally reconstructed Au(001) surface is particularly interesting because of the following reasons: (1) the top-most layer can be treated as an epitaxial layer in a lattice-mismatched interface; (2) existence of the rotated domains on the reconstructed surface must be clarified theoretically; (3) the experiments have predicted orientational phase transitions[13] but no clear theoretical explanation has been made. It is well understood that a Au(001) surface reconstruct to the $(5\times m)$ hexagonal layer where $m$ varies between 20 and 30. The top-most layer is contracted about 3.5%, slightly distorted, and buckled (but still shows epitaxial natures). Some x-ray experiments[13] have predicted the rotated domains with rotation angle $\theta\approx 0.5°$, 0.8°, and 1.0°. These domains undergo a phase transition around $T=0.75T_m$. However, other experiments[14] using an electron microscope have found a sheared lattice structure that might appear as a rotated domainlike image in an x-ray experiment. There are limited numerical molecular-dynamics simulation[15] and phenomenological studies[16] in the literature. The numerical simulation study is limited to a very small system size, and the phenomenological theory is based on a parametrized two-body potential at zero temperature in the limit of an infinite size system. Thus a more comprehensive explanation is necessary to understand the underlying physics of this subject.

To obtain a stable equilibrium configuration of a Au(001) surface we first examine various overlayer lattice structures at $T=0$ K. The hexagonal overlayer gives a lowest energy configuration. A limited sinusoidal corrugation is accommodated by considering the hexagonal overlayer mesh as two interpenetrating rectangular lattice meshes: the atomic positions are $(ib_{a,x},jb_{a,y})$, where $i(j)=\pm 1,\pm 3,\ldots,\pm(2n_x-1)$ $[\pm(2n_y-1)]$ for one rectangular mesh; and $i(j)$

$=0,\pm 2,\pm 4,\ldots,\pm 2n_x(\pm 2n_y)$ for the other. The former $(2n_x\times 2n_y)$ mesh is $\delta z$ above the other $(2n_x+1)\times(2n_y+1)$ mesh. The $(b_{a,x},b_{a,y})$ is a primitive lattice constant vector of the hexagonal overlayer lattice. The height of the overlayer atoms are either $z$ or $z+\delta z$ alternatively (hence the name of the ''*limited sinusoidal corrugation*''). More general corrugation can be accommodated by dividing the hexagonal lattice into a larger number of the rectangular meshes. However, for the sake of simplicity, we include this general corrugation effect in two adjustable free parameters that will be introduced in a later paragraph. Here the normal to the surface is defined as the $z$ axis, and the [10] direction of the square lattice and the [11] direction of the overlayer [along the ''5'' direction in the $(5\times m)$ reconstruction pattern] are chosen to be $x$ axes of the substrate and the overlayer, respectively.

The vibrational frequency of the substrate is calculated considering the overlayer as a laterally uniform (averaged over the layer) external charge and potential bath at the static equilibrium distance. The finite-size effects of the overlayer in the vibrational frequency are also neglected. We expect that the error involved in this approximation is less than few percents,[17] and mostly on the high-frequency region where the contribution to the free energy is less significant. Similarly the vibrational frequency of the overlayer lattice is calculated considering the substrate as an external bath at layer distance $z$. In this way the frequency depends only on the lattice constants $\vec{b}_a$, $\vec{b}_s$, and $z$. The substrate lattice constant $\vec{b}_s$ is calculated as a function of temperature by minimizing the substrate free energy, and thermal expansion similar to the previous study[11] is found.

For the interpenetrating rectangular overlayer mesh the interfacial free energy $F_{\rm int}^{(\rm tot)}$ is written as

$$
\begin{aligned}
F_{\rm int}^{(\rm tot)} &= \Phi_a(\vec{b}_a)+F_a^{(\rm vib)}(\vec{b}_a,z_e,T)\\
&\quad+\sum_{\vec{G}}\Gamma'_{\vec{G}}(z_e,\rho_{aa})\Delta_R(2n_x+1,2n_y+1,\vec{b}_a,\vec{G},\theta)\\
&\quad+\sum_{\vec{G}}\Gamma'_{\vec{G}}(z_e+\delta z,\rho_{aa})\Delta_R(2n_x,2n_y,\vec{b}_a,\vec{G},\theta)\\
&\quad+\sum_{\vec{K}}\Gamma_{\vec{K}}(z_e,\eta\rho_{ss})\Delta_R(n_x^{\rm eff},n_y^{\rm eff},\vec{b}_s,\vec{K},-\theta), \qquad (4)
\end{aligned}
$$

where $\Gamma'_{\vec{G}}(z_e,\rho_a)=V_{\vec{G}}+\Gamma_{\vec{G}}(z_e,\rho_a)$, $z_e=z+z_0$ is the effective layer distance, and $(n_x^{\rm eff}n_y^{\rm eff})$ is a number of the substrate atoms that are within interaction range of the overlayer. The geometric function $\Delta_R(n_x,n_y,\vec{b},\vec{G},\theta)=[\sin(n_xp)/\sin p][\sin(n_yq)/\sin q]\exp(i\vec{G}\cdot\vec{r}_0)$, where $p=(G_x\cos\theta+G_y\sin\theta)b_x/2$, $q=(-G_x\sin\theta+G_y\cos\theta)b_y/2$, and $\vec{r}_0$ is origin of the overlayer with respect to the substrate.[5] Here we introduce two free parameters $\eta$ and $z_0$ that are adjusted to be $\eta=0.935$ and $z_0=-0.0285$ Å by comparing the interface energy and the interface layer distance $z$ to a molecular-dynamics simulation result for $n_x=n_y=25$.[12] By minimizing this free energy with respect to the overlayer lattice constants $(b_{a,x},b_{a,y})$, the relative orientation $\theta$, the layer distance $z$, and the corrugation $\delta z$, we obtain a stable equilibrium configuration at a given temperature $T$ and the substrate lattice constant $\vec{b}_s$.

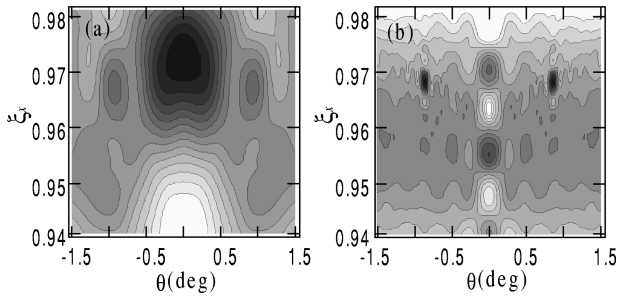


FIG. 1. The contour plots of $F_{\rm int}^{(\rm tot)}$ as a function of the overlayer lattice constant ratio $\xi_x$ and the relative orientation $\theta$ at $T=300$ K for (a) $n_x=10$, $n_y=40$ (80×230 Å); (b) $n_x=38$, $n_y=152$ (310×880 Å). The darker area represents the lower free energy.

In Fig. 1 we show the contour plots of the interfacial free energy $F_{\rm int}^{(\rm tot)}$ as a function of the lattice constant ratio $\xi_x$ $(=b_{a,x}/b_{s,x})$ and the relative orientation $\theta$ at $T=300$ K for: $n_x=10$, $n_y=40$ ($\approx$80×230 Å) in (a), and $n_x=38$, $n_y=152$ ($\approx$310×880 Å) in (b). The best values for the other parameters are $z=2.14$ Å, $\delta z=0.1$ Å, $\xi_y=0.951$ for the $n_x=10$ configuration, and $z=2.136$ Å, $\delta z=0.1$ Å, $\xi_y=0.957$ for the $n_x=38$ configuration. The minimum free energies per overlayer atoms are found to be $-3.965$ eV for $n_x=10$, $n_y=40$ cluster and $-4.132$ eV for $n_x=38$, $n_y=152$ cluster. A general feature in these figures is that the hexagonal overlayers are contracted and slightly distorted, i.e., the contraction ratios are about 3.3% ($\xi_x=0.967$) and 4.3% ($\xi_y=0.957$) in the $x$ and $y$ direction of the $n_x=38$ configuration, respectively. The contraction ratios for the $n_x=10$ configuration are 2.9% ($\xi_x=0.971$) in the $x$ direction and 4.9% ($\xi_y=0.951$) in the $y$ direction. An interesting feature in this figure is that a rotated phase ($\theta=\pm 0.86°$) is a stable phase for the larger cluster [Fig. 1(b)]. We find three rotated domains with rotation angles $\theta\approx\pm 0.72°$, $\pm 0.86°$, and $\pm 1.14°$ for cluster size $n_x\geqslant 35$ ($\approx$285 Å). This rotation angle is found to be related to the overlayer contraction ratio and, hence, the reconstruction pattern, i.e., for instance, $\theta=0.72°$, 0.86°, and 1.14° correspond to (5×28), (5×23), and (5×18) patterns, respectively. Similar relationship has been found in the two-body interaction potential model calculation at zero temperature.[16] Since the size of the overlayer cluster may affect the contraction ratio, the rotation angle differs in different overlayer geometry. In experiments there are many clusters with different shapes and sizes on a Au(001) surface. Thus all these three rotated domains as well as the unrotated domain are expected to be observed simultaneously at low temperatures in an experiment. Our calculated rotation angles are slightly larger than experimental values ($\pm 0.5°$, $\pm 0.8°$, and $\pm 1.0°$).[13] We think this slight discrepancy is due to inaccuracy of the interaction potential and/or the approximations in our model, and can be improved by using a more accurate interaction potential and/or including higher-order correction terms.

These rotated domains undergo the phase transformations from a rotated phase to another rotated phase or to an unrotated phase, as temperature increases. In Fig. 2 the interfacial free energy $F_{\rm int}^{(\rm tot)}$ is plotted as a function of the relative ori-

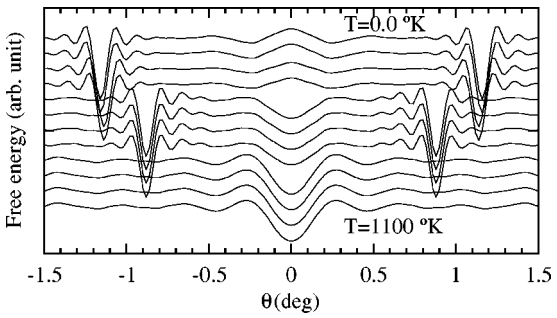


FIG. 2. The interfacial free energy $F_{\rm int}^{(\rm tot)}$ for a $n_x=40$ and $n_y=160$ (325×925 Å) cluster as a function of relative orientation $\theta$ at various temperatures.

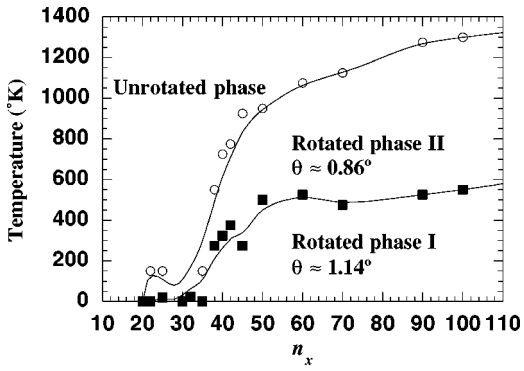


FIG. 3. The phase diagram for the orientational phase transitions. Here $n_y=4n_x$. The lines are guides to the eye.

entation $\theta$ for $n_x=40$ cluster at temperatures between $T=0$ K and 1100 K with 100 K increment. There are two phase transformations in this figure: one from $\theta=1.14°$ to 0.86° at $T\approx 300$ K, and the other from $\theta=0.86°$ to 0.0° at $T\approx 800$ K. The transitions seem to be first-order transition but our current calculation is not able to predict the exact type of the transition. Since all three rotated domains coexist at low to intermediate temperature regions due to many different sizes and shapes of clusters on a surface, and the transition looks more like first order, it may be difficult to observe the transition from one rotated domain to another rotated domain (*rotated-to-rotated*) in an x-ray experiment. As mentioned above the rotation angle is related to the reconstruction pattern and, consequently, an orientational phase transformation may be accompanied by a pattern transformation. We note here that choice of the free parameter $\eta$ may affect the transition temperature but the qualitative features does not change.

In Fig. 3 we plot a typical phase diagram that shows both the *rotated-to-rotated* and the *rotated-to-unrotated* phase transformations. The cluster in this diagram is a rectangular shape whose atomic rows in the $y$ direction are four times that in the $x$ direction. For a cluster smaller than $n_x\approx 25$ ($\approx$205×580 Å) an unrotated phase is only a stable phase at all temperatures. However for larger clusters rotated phases are stable in the low temperature whereas an unrotated phase is the stable one in the high-temperature region. Thus an experiment may observe the phase transformations at temperature below the bulk melting temperature, since a typical size of terrain on the surface has been measured to be larger than 300 Å in the experiments.[13,14] The transition temperature varies with the cluster size and saturates at $n_x\geqslant 90$ to a temperature close to the melting temperature. Considering that a typical cluster size in an experiment is few hundreds angstrom, the experimental transition temperature 970 K is within our predicted range but a direct comparison with experimental values is not possible due to a lack of experimental studies of size-dependent orientational phase transition in the literature. Other shapes of clusters may show different phase diagrams (for instance, there is no rotated-to-rotated phase transformation in a square type cluster) but general features are similar to the above. Further detail on this matter will be discussed elsewhere.[12]

In conclusion we have developed a theoretical approach in studying epitaxy in lattice-mismatched interfaces at finite temperatures. An application of this theory to Au(001) surface reconstruction predicts correctly the experimentally observed rotated domains. These rotated domains undergo the orientational phase transformations accompanied by the simultaneous pattern transformations at temperatures below the melting temperature. Our predictions are in very good agreement with the available experiments.[13]

This work was supported by the KOSEF through ASSRC. We thank SERI for supercomputer time.

[1] See, for example, *Epitaxial Growth*, edited by J. W. Mathews (Academic, New York, 1975); B. A. Joyce, in *Molecular Beam Epitaxy and Heterostructures*, edited by L. L. Chang and K. Ploog, Vol. 87 of *NATO Advanced Study Institute, Series E: Applied Sciences* (Plenum, New York, 1985); J. A. Venables, Vacuum **33**, 701 (1983).

[2] See, for instance, various articles in MRS Bull. **8** (1988).

[3] For a comprehensive list of epitaxial systems, see E. Grünbaum, in *Epitaxial Growth* (Ref. 1), p. 611.

[4] A. Kobayashi and S. Das Sarma, Phys. Rev. B **35**, 8042 (1987); R. Ramirez, A. Rahman, and I. K. Schuller, *ibid.* **30**, 6208 (1984); L. A. Bruce and H. Jaeger, Philos. Mag. A **38**, 223 (1978); L. W. Bruch, Surf. Sci. **250**, 267 (1991).

[5] J. H. van der Merwe and M. W. H. Braun, Appl. Surf. Sci. **22/23**, 545 (1985); J. H. van der Merwe, Philos. Mag. A **45**, 127 (1978); **45**, 159 (1978); S. M. Paik and I. K. Schuller, Phys. Rev. Lett. **64**, 1923 (1990).

[6] A. Madhukar and S. V. Graisas, CRC Crit. Rev. Solid State Mater. Sci. **14**, 1 (1988); A. Kobayashi and S. Das Sarma, Phys. Rev. B **37**, 1039 (1988).

[7] S. M. Paik and S. Das Sarma, Phys. Rev. B **39**, 1224 (1989); M. Schneider, I. K. Schuller, and A. Rahman, Phys. Rev. Lett. **55**, 604 (1985); Phys. Rev. B **36**, 1340 (1987).

[8] Y. Qian, M. J. Bedzyk, S. Tang, A. J. Freeman, and G. E. Franklin, Phys. Rev. Lett. **73**, 1521 (1994).

[9] W. Jones and N. H. March, *Theoretical Solid State Physics* (Dover Publication, New York, 1985), Vol. 1, p. 236.

[10] M. I. Baskes, Phys. Rev. B **46**, 2727 (1992); M. I. Baskes, M.

Daw, B. Dodson, and S. Foiles, MRS Bull. **13**, 28 (1988).
[11] F. Ercolessi, M. Parrinello, and E. Tosatti, Philos. Mag. A **58**, 213 (1988).
[12] S. M. Paik *et al.* (unpublished).
[13] G. M. Watson, D. Gibbs, D. M. Zehner, M. Yoon, and S. G. J. Mochrie, Phys. Rev. Lett. **71**, 3166 (1993); S. G. J. Mochrie, D. M. Zehner, B. M. Ocko, and D. Gibbs, *ibid.* **64**, 2925 (1990); K. Yamazaki, K. Takayanagi, Y. Tanishro, and K. Yagi, Surf. Sci. **199**, 595 (1988).
[14] D. N. Dunn, J. P. Zhang and L. D. Marks, Surf. Sci. **260**, 220 (1992).
[15] X. Q. Wang, Phys. Rev. Lett. **67**, 3547 (1992).
[16] Y. Okwamoto and K. H. Bennemann, Surf. Sci. **179**, 231 (1987).
[17] The first-order correction term due to the lateral periodicity is an order of $\sim\alpha|k|b$ where $\alpha=0.0567$ for a typical lattice; A. A. Maradudin, in *Physics of Phonon*, edited by T. Paszkiewicz, Lecture Notes in Physics Vol. 285 (Springer-Verlag, New York, 1987), p. 82; B. Djafari-Rouhani and L. Dobrzynski, Surf. Sci. **110**, 129 (1981); for the finite-size effects, see for example, C. Koziol, J. P. Toennies, and G. Zhang, in *Phonons 89: Proceedings of the Third International Conference on Phonon Physics*, edited by S. Hunklinger, W. Ludwing, and G. Weiss (World Scientific, Singapore, 1990), p. 880.